Top Catal (2015) 58:1193–1201
DOI 10.1007/s11244-015-0491-9

ORIGINAL PAPER

Reaction Rate Enhancement During the Electrocatalytic Synthesis of Ammonia in a $BaZr_{0.7}Ce_{0.2}Y_{0.1}O_{2.9}$ Solid Electrolyte Cell

E. Vasileiou[1,2] · V. Kyriakou[1,2] · I. Garagounis[1,2] · A. Vourros[1,2] · A. Manerbino[3] · W. G. Coors[3] · M. Stoukides[1,2]

Published online: 14 September 2015

Abstract The catalytic and electrocatalytic synthesis of ammonia was studied in a proton conducting double-chamber solid electrolyte cell. The $BaZr_{0.7}Ce_{0.2}Y_{0.1}O_{2.9}$ (BZCY72) proton conducting ceramic was used as the electrolyte with a Ni-BZCY72 cermet and a Pt film serving as cathodic and anodic electrodes, respectively. The reaction was studied at atmospheric pressure and at temperatures between 450 and 700 °C, under both, open- and closed-circuit conditions. A peculiar reaction rate enhancement was observed when the cell returned to open-circuit after operating under closed-circuit for a certain time. A possible explanation of this new phenomenon is that a fraction of protons electrochemically transported to the cathode, is "stored" in the Ni-BZCY72 electrode in the form of a highly reactive hydride which, upon current interruption, reacts with adsorbed N species to produce ammonia.

Keywords Ammonia synthesis · Proton conducting cells · Post-electrochemical reaction rate enhancement

1 Introduction

The dominant route to the production of ammonia from its elements is the Haber–Bosch process, which involves the reaction of N_2 and H_2 on a Fe-based catalyst at temperatures between 400 and 500 °C and at pressures between 50 and 150 bar [1]. This reaction is considered a top scientific achievement of the twentieth century and a landmark in heterogeneous catalysis [1–4]. In order for industrially acceptable conversions to be achieved, problems of both thermodynamics and reaction kinetics have to be overcome. Gaseous N_2 is a very stable molecule and even the most efficient catalysts require operation at elevated temperatures. On the other hand, the reaction is exothermic and its equilibrium conversion decreases with temperature. Hence, to obtain the desired conversions to ammonia, high pressures must be employed in order to push the equilibrium to the right [4].

The Haber–Bosch process has been studied and improved for more than one hundred years. Active catalysts that permit operation at lower pressures have been introduced. Also, several alternative approaches have been proposed including the electrochemical synthesis [2–4]. In the latter, hydrogen and nitrogen are fed in over the anode and the cathode, respectively, of an electrochemical cell. Upon supply of electrical energy, hydrogen is converted into protons, which are transported to the cathode and react with nitrogen to produce ammonia. The discovery of solid state proton conductors in the early 80's [5] enabled operation at atmospheric pressure and temperatures of industrial interest (>400 °C). Thus, the feasibility of the above described "Solid State Ammonia Synthesis" (SSAS), was successfully demonstrated in 1998 [6]. Since then, research groups worldwide have contributed in identifying the means to promote SSAS to an industrial scale [2–4].

One basic requirement for SSAS is that the cathodic electrode must exhibit both catalytic activity towards ammonia synthesis and high electronic conductivity. Unfortunately, the industrial catalysts (either Fe- or Ru-based) contain various inorganic oxides and thus are very

✉ M. Stoukides
stoukidi@cperi.certh.gr

[1] Department of Chemical Engineering, Aristotle University, Thessaloniki, Greece

[2] Chemical Processes and Energy Resources Institute, CERTH, Thessaloniki, Greece

[3] CoorsTek Inc., Golden, CO 80401, USA

poor conductors. In a recent communication [7], it was reported that a Ni-based cermet of the form Ni-$BaZr_{0.7}Ce_{0.2}Y_{0.1}O_{2.9}$ (Ni-BZCY72) met the above two requirements in a satisfactory manner. The reaction was studied at atmospheric pressure and at temperatures between 450 and 650 °C in a single-chamber cell, i.e. an electrochemical cell in which both electrodes are exposed to the same reacting mixture. The electrocatalytic rate achieved in that cell (2.9×10^{-9} mol s^{-1} cm^{-2}) can be compared to the highest reported for electrochemical ammonia synthesis, which were of the order of 10^{-8} mol s^{-1} cm^{-2} [4, 7].

One advantage of the double versus the single chamber cell is that in the double the two electrode compartments are gas-tightly separated from each other and therefore, regardless of the hydrogen source, only protons (H^+) can be transported through the solid electrolyte. The cost for preparation and purification of the synthesis gas is a major factor in the overall economics of ammonia synthesis [1, 4]. Using double-chamber H^+ conducting cells, ammonia synthesis from H_2O, rather than H_2, has been reported by various research groups in the past decade [8–14]. Clearly, ammonia synthesis from nitrogen and water at atmospheric pressure with the use of electricity will constitute a potential economic and environmental breakthrough [15].

The present communication reports on the catalytic and electrocatalytic synthesis of ammonia in a double-chamber BZCY72 proton conducting cell. The high catalytic activity was observed again. Moreover, a peculiar reaction rate enhancement was observed when the cell returned to open-circuit after operating under closed-circuit for a certain time. This new phenomenon, currently named "Post Electrochemical Open Circuit Enhancement" (PELOCE), could potentially be of practical use.

2 Experimental

2.1 Cell Preparation

With the exception of the reactor-cell, the experimental apparatus used in this study was the same as that described in Ref. [7]. The reactor cell configuration is shown in Fig. 1 with the inset giving a more detailed picture of the various layers of the cell. It was a slip-cast, electrode-supported tube, 25 cm long, closed at one end, fabricated by CoorsTek (CoorsTek Inc., Golden, CO, USA). The dense electrolyte layer ($BaZr_{0.7}Ce_{0.2}Y_{0.1}O_{2.9}$ -BZCY72) had a thickness of 30 μm. A supporting porous electrode (65 wt% NiO-35 wt% $BaZr_{0.7}Ce_{0.2}Y_{0.1}O_{2.9}$) with a thickness of approximately 750 microns was placed inside the tube and served as the working electrode (cathode). A porous Pt film was deposited at the outside and served as counter electrode (anode). The counter electrode was prepared from Pt powder (Alfa Aesar # 12345) suspended in ethylene glycol (Baker Chemical). The superficial surface area of the Pt electrode was 8 cm^2. The sintering of the Pt electrode took place at 750 °C for 3 h under 25 mL min^{-1} flowing air, followed by reduction for 2 h in 30 mL min^{-1} of a 10 % H_2/N_2 mixture. The morphology and structure analysis of the fresh sample was carried out by scanning electron microscopy using a JEOL JSM 6300 microscope, equipped with an Oxford Instruments INCA x-sight detector for EDS measurements.

2.2 Reaction Kinetics and Electrochemical Measurements

The experiments were conducted under atmospheric pressure, at temperatures from 460 to 660 °C. The volumetric

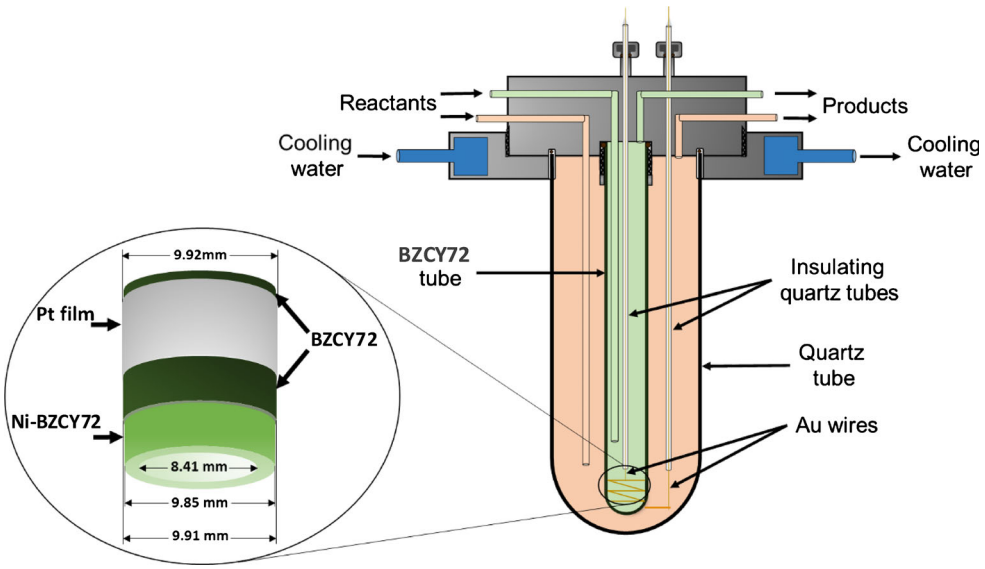

Fig. 1 Illustration of the double-chamber reactor cell

flowrate was kept at 150 mL min^{-1} in each chamber via mass-flow controllers (Bronkhorst High Tech). The reactant gases, H_2 and N_2, were certified high purity standards (99.999 %, Air Liquide-Hellas). Hydrogen concentrations were measured via online gas chromatography using a SHIMADZU GC 14B chromatograph equipped with a Molecular Sieve 5A column with N_2 as a carrier gas. The produced ammonia was measured by an EAA-24r-EP (Los Gatos Research, Mountain View, CA) real time analyzer operating with the cavity ringdown spectroscopy (CRDS) technique. Constant voltages were imposed across the cell using an AMEL 7050 galvanostat–potentiostat.

3 Results

3.1 Morphological Analysis

SEM pictures of the Ni-BZCY72 cermet cathode (inside surface of the tube) and of the cross-section of Ni-BZCY72 and BZCY72 electrolyte are shown in Fig. 2, for a fresh sample after reduction at 750 °C in 10 % H_2/N_2. The images reveal a relatively modest porosity of the Ni-BZCY72 (Fig. 2a) and excellent adherence between the 30 μm solid electrolyte and the high thickness porous cathodic electrode (Fig. 2b).

3.2 Catalytic (Open-Circuit) Experiments

In order to test the catalytic activity of the Ni-BZCY72 electrode, experiments were first conducted under open-circuit (i.e. I = 0). In Fig. 3a, the reaction rate is plotted against the inlet P_{H2}/P_{N2} ratio, at temperatures between 580 and 660 °C. Better performances were observed at the feed ratio $P_{H2}/P_{N2} = 3$ at higher temperatures, while at 580 °C, the best performance was obtained at a feed ratio of 1.0.

Figure 3b shows the dependence of the rate of NH_3 synthesis on temperature for various H_2/N_2 feed ratios. For all reactant gas compositions, the maximum reaction rate is attained at temperatures near 620 °C. Experimental results, similar to those reported here, were obtained with the Rh/BZCY72/Ni-BZCY72 single-chamber cell [7]. Because of its single-chamber configuration, however, both Rh and Ni-BZCY72 were exposed to the reacting mixture. The present results prove conclusively that the Ni-BZCY72 cermet is a very active catalyst for NH_3 synthesis.

3.3 Electrocatalytic (Closed-Circuit) Experiments

The closed-circuit experiments were conducted at temperatures between 450 and 700 °C and atmospheric total pressure. Pure H_2 was introduced over the Pt electrode and a mixture of H_2 and N_2 (instead of N_2 only) was introduced over the Ni-BZCY72 electrode. The introduction of a H_2–N_2 mixture (rather than N_2 alone) was dictated by previous works [7, 16], in which it was found that, for a measurable rate of NH_3 formation to be obtained, a minimum hydrogen content (>1 %) is required at the cathode side.

Figures 4a, b show the effect of applied voltage on the rate of NH_3 synthesis for $P_{H2}/P_{N2} = 1$ and $P_{H2}/P_{N2} = 3$, respectively. The experiments of Fig. 4 were conducted as follows: First, an open circuit steady state was established and the reaction rate was measured. The steady state open-

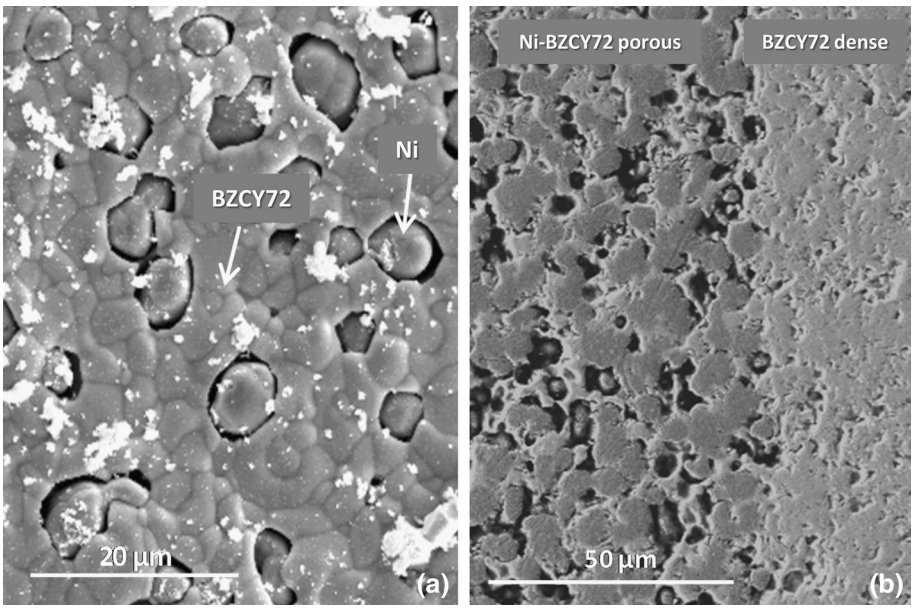

Fig. 2 SEM images of the **a** Ni-BZCY72 cermet surface and **b** cross-section of the BZCY72/Ni-BZCY72 interphase

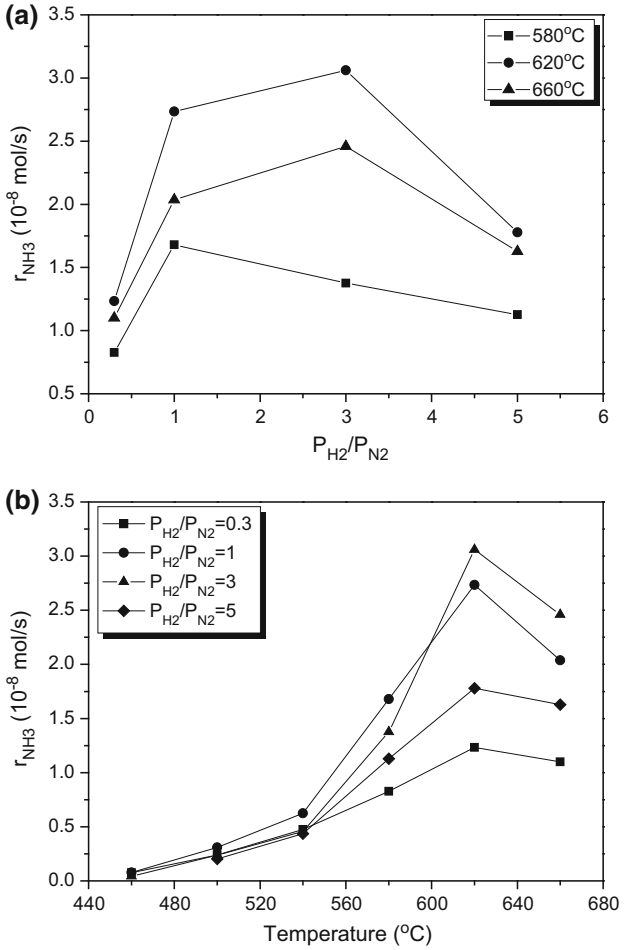

Fig. 3 Dependence of the open-circuit rate of NH_3 formation on the P_{H2}/P_{N2} feed ratio (**a**) and on temperature (**b**)

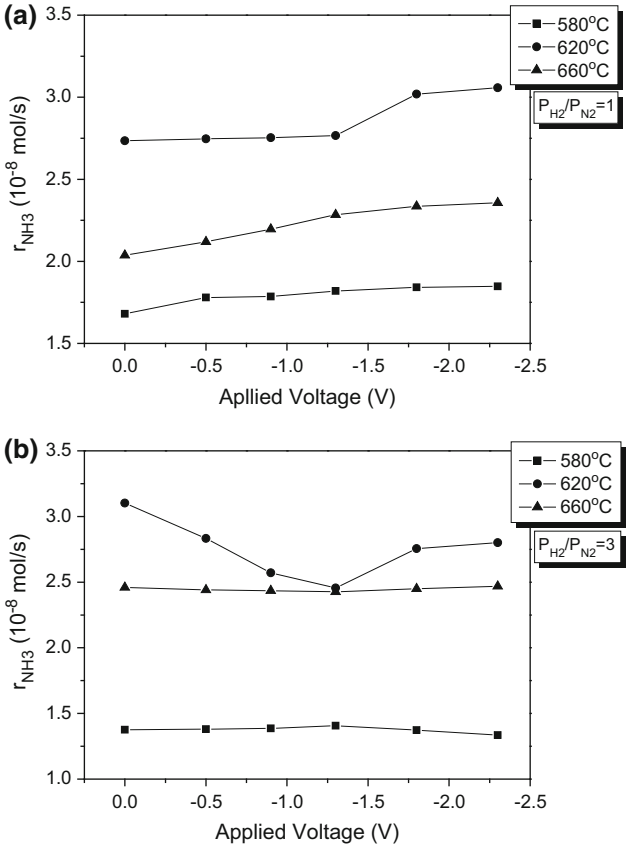

Fig. 4 Dependence of the NH_3 formation rate on the applied voltage **a** $P_{H2}/P_{N2} = 1$ and **b** $P_{H2}/P_{N2} = 3$

circuit rates are shown on the vertical axis, i.e. for V = 0.0. Then, the circuit was closed and a constant voltage was applied across the cell. The voltage was considered negative when protons were transferred from the Pt surface to the Ni-BZCY72 cermet electrode. After a short period (5–15 min), a new steady state was established and these closed-circuit steady state rates are the data points of Fig. 4. It can be seen that the applied voltage can increase the ammonia formation rate by up to 15 % for $P_{H2}/P_{N2} = 1.0$ (Fig. 4a). A minute enhancement (at 580 °C) and even a decrease (at 620 °C) in the reaction rate is observed for $P_{H2}/P_{N2} = 3.0$ (Fig. 4b).

3.4 Post Electrochemical Open Circuit Enhancement (PELOCE)

Figures 5, 6, 7, 8, and 9 present the experimental characteristics of PELOCE, a phenomenon not reported before. In Fig. 5a, the rate of NH_3 synthesis and the cell voltage are plotted versus time. First, the cell operated at open circuit. A mixture of H_2 and N_2 ($P_{H2}/P_{N2} = 1.0$) and a pure H_2 stream were introduced over the Ni-BZCY72 and the Pt electrode, respectively. A steady state was established and the measured reaction rate was equal to 1.54×10^{-8} mol/s. At t = 20 min, the circuit was closed and a constant voltage of −1.5 V was imposed. A small increase in the reaction rate was observed and a new steady state value was soon established (1.56×10^{-8} mol/s). At t = 50 min., the cell voltage was changed to −2.0 V and the reaction rate gradually attained a new slightly higher steady state value. Similarly, at t = 80 min., the voltage changed to −2.5 V and the reaction rate gradually leveled off at 1.67×10^{-8} mol/s, which corresponds to an 8.3 % increase in the open-circuit rate. At t = 110 min, the circuit was opened.

Figure 5b shows in more detail the transient reaction rate and voltage behavior. Upon opening the circuit, the cell voltage dropped abruptly to −280 mV. In the next 50 min, the voltage dropped to close to −15 mV. During that period, instead of decreasing, the reaction rate increased and reached a maximum of 2.25×10^{-8} mol/s, corresponding to a 44.7 % increase over the initial open-circuit rate. After a period of about 15 min, during which

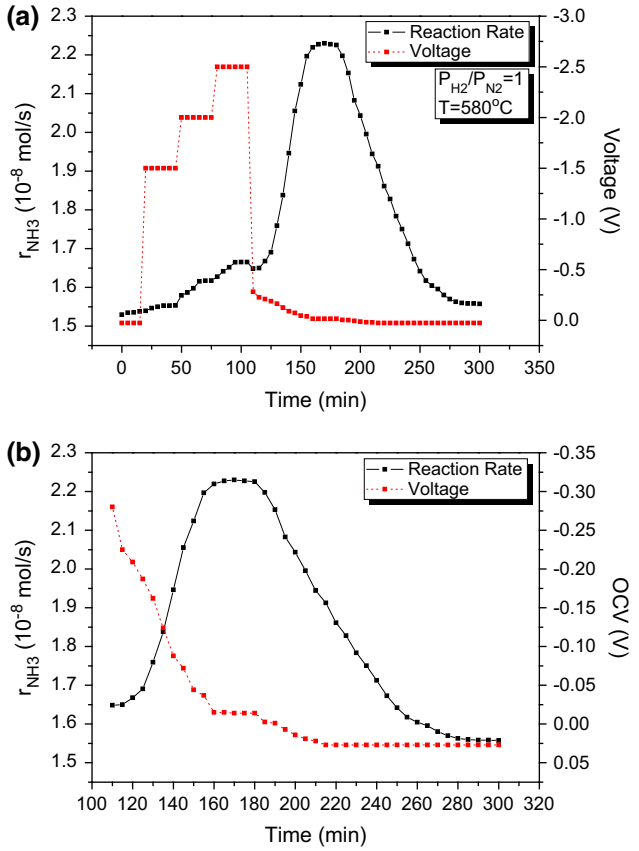

Fig. 5 NH_3 formation rate and cell voltage transients for **a** the entire experiment ($0 < t < 300$) and **b** after opening the circuit ($110 < t < 300$)

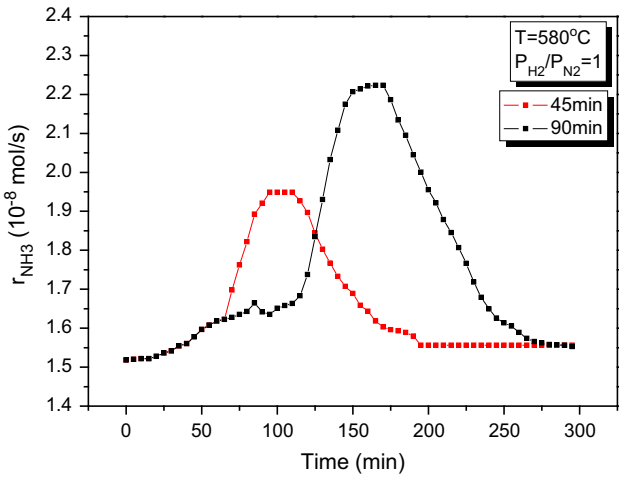

Fig. 6 Dependence of reaction rate transients after opening the circuit on duration of preceding galvanostatic operation (I = 150 mA)

both remained essentially unchanged (Fig. 5b), both, rate and voltage began to decrease slowly to reach their original values after about 100 min.

In Fig. 6, the above described phenomenon is shown for two experiments in which the reactant composition, the

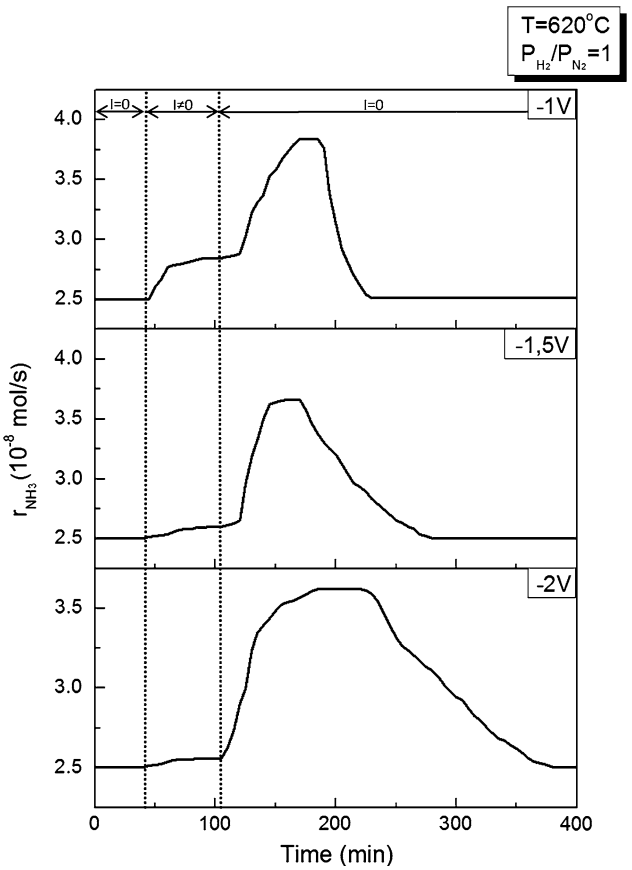

Fig. 7 NH_3 formation transients under different applied voltages at 620 °C. The corresponding transported electric charge was **a** 295 Coulomb, **b** 522 Coulomb and **c** 911 Coulomb

operating temperature and the applied current were kept constant at $P_{H2}/P_{N2} = 1.0$, T = 580 °C and I = 150 mA, respectively. The two experiments differed in the "pumping" time, which was 45 and 90 min for the red and the black data points, respectively. Figure 6 shows a 28.6 % and a 46.3 % reaction rate enhancement for the 45 and 90 min experiments, respectively. The areas under the two curves, which represent the increase in the moles of NH_3 produced, correspond to 18.9 and 37.4 μmoles, respectively. This implies that the reaction rate enhancement is nearly proportional to the time of closed-circuit operation, or, equivalently, to the total number of protons transferred to the cathode.

The dependence of the reaction rate on the applied voltage is shown in Fig. 7. Reactant composition and temperature were kept at $P_{H2}/P_{N2} = 1.0$ and T = 620 °C, respectively. The time of closed circuit operation was kept the same, while the applied voltage (and consequently the generated current) varied. At low voltage values, a more pronounced closed-circuit enhancement and a slightly higher post electrochemical peak were observed. The duration of the PELOCE effect, however, increased with applied voltage reaching the 4.5 h (270 min) at −2 V. The

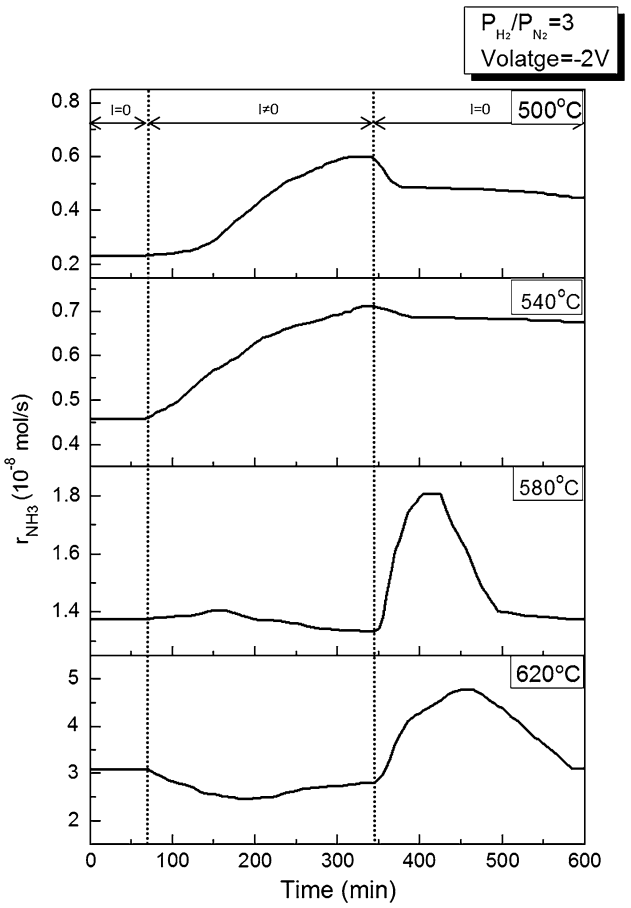

Fig. 8 Reaction rate transients at 500–620 °C for $P_{H2}/P_{N2} = 3$ and for 4.5 h (270 min) of operation under closed circuit

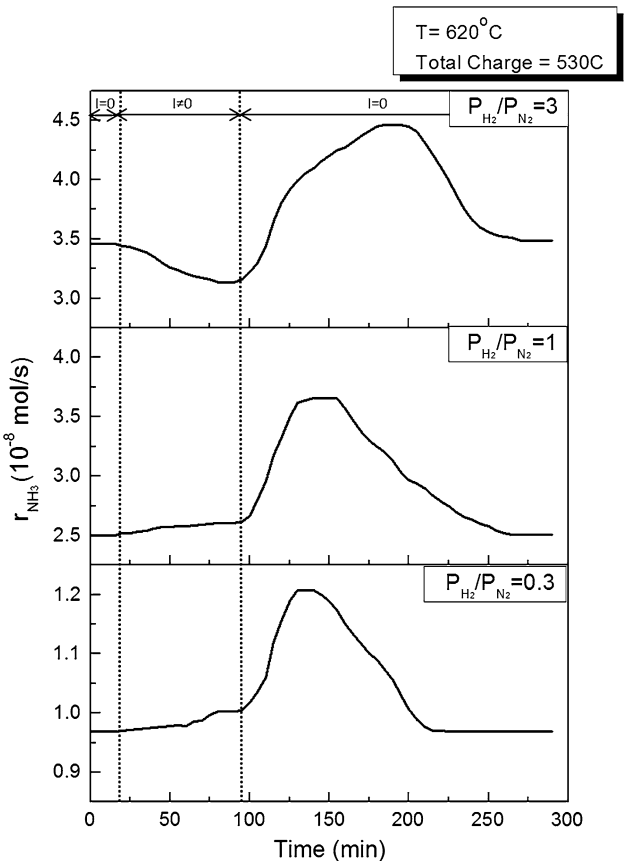

Fig. 9 Reaction rate transients at 620 °C for **a** $P_{H2}/P_{N2} = 3.0$, **b** $P_{H2}/P_{N2} = 1.0$ and **c** $P_{H2}/P_{N2} = 0.3$

total electric charge transported to the cathode was 295, 522 and 911 Coulombs for cases (a), (b) and (c), respectively. The areas under the three curves of Fig. 7, which again represent the increase in the produced moles of NH_3, correspond to 63.8, 83.3 and 100.5 μmol of NH_3, for cases (a), (b) and (c), respectively.

In Fig. 8 the PELOCE effect at temperatures between 500 and 620 °C and at stoichiometric inlet reactant composition ($P_{H2}/P_{N2} = 3.0$) is plotted against time, the applied voltage and the time of closed-circuit operation kept constant at −2.0 V and 4.5 h, respectively. It can be seen that, at 500 and 540 °C, a considerable increase in the reaction rate is attained under closed circuit and when the circuit is again opened, the rate drops only slightly and remains higher than its initial open circuit value for several hours. On the other hand, at 580 and 620 °C, the rate essentially decreased at closed circuit rate and exhibited a remarkable increase after the circuit is opened.

A comparison of the data at 580 °C in Figs. 5a and 8, reveals significant differences in the post-electrochemical rate enhancement between $P_{H2}/P_{N2} = 1.0$ and $P_{H2}/P_{N2} = 3.0$. Figure 9 shows the effect of reactant composition in which the reactant feed ratio affects the rate of ammonia synthesis both before and after current interruption. The low P_{H2}/P_{N2} feed ratio gave a more pronounced closed-circuit enhancement but a lower and narrower PELOCE peak. Conversely, at $P_{H2}/P_{N2} = 3.0$, a rate decrease occurred at closed circuit, while the PELOCE peak was both higher and broader. It should be pointed out that the reaction rate enhancement presented in Figs. 5, 6, 7, 8, and 9 is observed only after applying a negative voltage, i.e. pumping protons to the catalyst. When protons are pumped away from the catalyst, a slight decrease in the reaction rate is observed and then, upon current interruption, the rate gradually returns to its initial open-circuit value.

4 Discussion

The open circuit results verified the high catalytic activity of Ni towards NH_3 synthesis, first observed in a single-chamber cell of the form Rh/NiBZCY72/Ni-BZCY72 [7]. Metallic nickel is not among the best catalysts for ammonia

synthesis [1], but is significantly promoted when in the lattice of perovskite materials [17, 18].

Moreover, the constituents of the BZCY72 electrolyte are reported to catalyze efficiently the dissociation of molecular nitrogen [1]. Barium is a promoter for the industrial catalysts [1, 19] while Zr and Y are reported to bind atomic nitrogen at the expense of hydrogen [20]. In a recent work, in which ammonia synthesis was studied on Ru using various supports, it was found that, when Ru was supported on $BaZrO_3$, the reaction rate was much higher than that on any other support, including carbon material systems [21].

The positive effect of the solid electrolyte materials has also been proposed to explain the high catalytic activity of Ag and Pd electrodes [4]. Palladium and silver are poor catalysts for ammonia synthesis. In most of the studies of electrochemical synthesis of NH_3, however, a Pd–Ag electrode was successfully used [4]. On the other hand, the solid electrolytes that were used in these works contained early transition metals such as Sc, Y, Ti and Zr, which exhibit high catalytic activity. Thus, it may be considered a fortunate coincidence that the constituents of the H^+ solid electrolyte act as catalyst promoters.

In the last 3 decades, solid electrolyte cells have been used as cell-reactors in which heterogeneous catalytic reactions were studied. When the circuit is open and the reactant gases are fed in together, the cell behaves as a regular catalytic reactor in which the catalyst is the working electrode. When the circuit is closed and a constant voltage (or a constant current) is applied, the cell can additionally function as an electrochemical ion "pump". If, for example, a proton (H^+) conductor is used, the current, I, corresponds to I/2F moles of hydrogen per second transported through the electrolyte. If r_o and r are the open- and closed-circuit reaction rates respectively (expressed in mol of hydrogen/s), two dimensionless numbers, Λ and ρ, can be used to evaluate the electrochemical enhancement of the reaction rate [22, 23], defined as:

$$\Lambda = \Delta r/(I/2F) = (r - r_o)/(I/2F) \quad (1)$$

and

$$\rho = r/r_o \quad (2)$$

If $\Lambda = 1$, the effect is Faradaic, i.e. the increase in reaction rate equals the rate of ion transport through the electrolyte. In numerous catalytic systems, however, the phenomenon of Non-Faradaic Electrochemical Modification of Catalytic Activity (NEMCA), also called Electrochemical Promotion of Catalysis (EPOC), has been observed [22–24], i.e. Λ exceeded unity. Values of Λ as high as of the order of 10^5 have been reported in certain catalytic reactions such as the oxidation of ethylene on Pt [22–24]. Significantly lower values, however, have been observed in the reaction of NH_3 synthesis in H^+ conducting cells [25–27].

The electrocatalytic results presented in Fig. 4a show an apparently weak effect of proton "pumping" on the reaction rate (low ρ values). It should be pointed out, however, that the open-circuit rates were very high. This, in turn, is due to the high catalytic surface area of the Ni-BZCY72 cermet. For example, at 620 °C, the open circuit rate is 2.7×10^{-8} mol/s and upon application of -2.4 V, it increases to 3.1×10^{-8} mol/s (Fig. 4a). This gives a net electrocatalytic rate of 4.0×10^{-9} mol/s or, 0.5×10^{-9} mol/s cm^2 (dividing by the area of the Pt electrode), which is considered as a modest electrocatalytic NH_3 synthesis rate [4]. On the other hand, the values of Λ, calculated for the data of Fig. 4a, are very poor ($\Lambda < 1$). There are two factors contributing to this undesirable result. First, the reaction kinetics; even when protons are used instead of gaseous hydrogen, it is difficult to combine with nitrogen. Most of the supplied protons combine with each other to produce molecular H_2. Second, thermodynamics; the equilibrium conversion of this reaction is limited. As opposed to reactions with highly negative free energy change (e.g. oxidation of hydrocarbons), in which Λ values of the order of 10^5 have been reported [22–24], in reactions of limited thermodynamic conversion the effect of H^+ pumping is both, electrochemical and catalytic and thus, even if the kinetic problems are completely eliminated, the Λ values would hardly exceed unity ($\Lambda < 3.0$) under these conditions [25].

Figure 4b shows that proton "pumping" has essentially a negative effect on the reaction rate. The experimental conditions differed from those of Fig. 4a only in the reactant composition (P_{H2}/P_{N2} was 1.0 and 3.0 in Fig. 4a, b, respectively) and therefore, the decrease in the reaction rate should be associated to the increase in the H_2/N_2 ratio over the cathode. Hydrogen and nitrogen adsorb competitively on the catalyst surface and a proton flux acts as a poison for nitrogen chemisorption. Similar phenomena have been reported in previous studies of the electrochemical synthesis of ammonia [2, 4, 28]. Wang et al. studied the effect of applied current and found that at low current values, the reaction rate increased with current up to a certain value above which a significant decrease was observed [28].

The post-electrochemical phenomena on the reaction rate, presented in Figs. 5, 6, 7, 8, and 9 can be compared to those reported previously in catalytic studies conducted in solid electrolyte cells. In Fig. 10, the effect of ionic "pumping" on the catalytic reaction rate is plotted versus time in three different cases. The first case (Fig. 10a) is the classic type of behavior, according to which the initial open circuit rate is enhanced upon closing the circuit and when the circuit is opened again, the rate quickly returns to its

previous value [22–24]. In the second case (Fig. 10b), upon closing the circuit, the reaction rate increases to a new steady state value but when the circuit is opened again, the rate does not return to its initial value for several (8–10) hours. This phenomenon is known as "permanent NEMCA" and has been studied in detail by Comninelis and co-workers [29–32]. Finally, Fig. 3c shows the PELOCE effect, presented in this work.

The experimental findings of PELOCE can be summarized as follows.

(a) The reaction rate is enhanced only after operating the cell under closed-circuit and in the direction of supplying protons to the catalyst surface.
(b) A minimum temperature is required for the phenomenon to appear. At lower temperatures the reaction rate does not exceed its closed circuit value; it just takes longer to return to the initial steady state (Fig. 8).
(c) The reaction rate enhancement is nearly proportional to the number of protons transferred to the cathode during closed-circuit operation (Fig. 6).

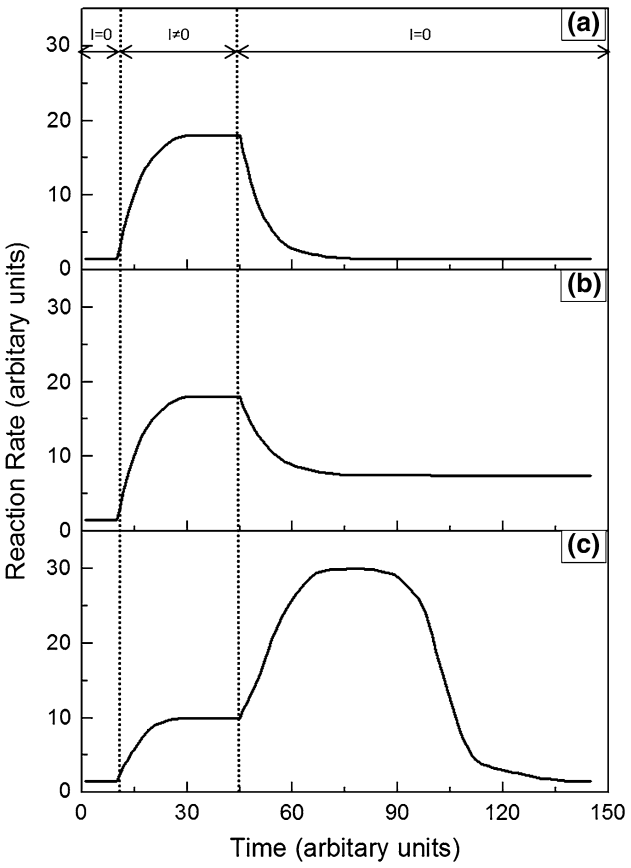

Fig. 10 Reaction rate transients during electrochemical ionic "pumping". **a** Classic behavior, **b** permanent NEMCA, **c** post-electrochemical open-circuit enhancement

(d) An increase in the P_{H2}/P_{N2} ratio is followed by an increase in both rate enhancement and additional number of moles of ammonia produced (Fig. 9).

PELOCE seems to have similarities to the "Permanent NEMCA" effect of Fig. 10b. Falgairette et al. [30] studied the latter in detail and reported delayed oxygen storage at the metal-electrolyte interphase. The oxygen species were thus "hidden" from the gas phase and were released during relaxation time [30]. This pseudo-capacitive behavior of the cell could be the explanation of the PELOCE effect. More specifically, a fraction of the protons that reach the cathode is "stored" at the Ni-BZCY72 interphase in the form of Ni–H species, probably as a Ni_xH_y hydride. The Ni hydride is formed only under electrochemical proton pumping. Upon current interruption, the hydride reacts readily with nitrogen to form ammonia. The rate increase is not observed under closed-circuit because nitrogen chemisorption is hindered by the H^+ flux. This scheme can also explain the lack of rate enhancement observed in certain experiments (Figs. 8 and 9a).

In summary, the present work can be considered as a positive addition to the development of an efficient SSAS process. The double-chamber BZCY72/Ni-BZCY72 cell exhibits a number of advantageous characteristics. First, steam instead of hydrogen can be used as a reactant without poisoning the catalyst. Second, the 30 micron thickness of the solid electrolyte allows for high H^+ fluxes. Third, the Ni-BZCY72 cermet exhibits both high electronic conductivity and catalytic activity. Recent studies recommend the use of metal nitrides as working electrodes [15, 33, 34]. To partially or fully replace nickel by molybdenum or iron nitride will be a difficult task, but it may be worth the challenge.

5 Conclusions

The catalytic and electrocatalytic synthesis of ammonia was studied in a proton conducting double-chamber $BaZr_{0.7}Ce_{0.2}Y_{0.1}O_{2.9}$ (BZCY72) solid electrolyte cell. The cathodic electrode, which was the catalyst for ammonia synthesis, was a Ni-BZCY72 cermet, while Pt served as the anode. The reaction was studied under atmospheric pressure and at 450–700 °C temperature range. The catalytic studies showed that Ni-BZCY72 is active for ammonia synthesis with the highest observed formation rate being 3.1×10^{-8} mol/s. Under closed-circuit and by pumping protons to the catalyst a moderate increase of 4×10^{-9} mol/s was observed in the reaction rate. At the higher temperatures tested (>620 °C) the current had no effect on the open-circuit rate of ammonia until the circuit was opened again. A PELOCE was observed with an up to

40 % enhancement of the initial open-circuit rate. The PELOCE phenomenon reported herein is interesting from both a theoretical and a practical point of view. Additional experiments should be designed in order to elucidate its origin. If exploitable, this phenomenon could add to the promotion of SSAS into industrial practice.

Acknowledgments We gratefully acknowledge financial support of this research by the European Union and the General Secretariat of Research and Technology of Greece (Program ARISTEIA, Project Number 1089),as well as by the IKY fellowships of excellence for postgraduate studies in Greece - Siemens Program.

References

1. Liu H (2014) Chin J Catal 35:1619–1640
2. Amar IA, Lan R, Petit CTG, Tao SW (2011) J Sol St Electrochem 15(9):1845–1860
3. Giddey S, Badwal SPS, Kulkarni A (2013) Int J Hydrog Energy 38(34):14576–14594
4. Garagounis I, Kyriakou V, Skodra A, Vasileiou E, Stoukides M (2014) Front Energy Res 2:1–10
5. Iwahara H, Esaka T, Uchida H, Tanaka N (1981) Solid State Ion 3/4:359363
6. Marnellos G, Stoukides M (1998) Science 282:98–100
7. Vasileiou E, Kyriakou V, Garagounis I, Vourros A, Stoukides M (2015) Solid State Ion. doi:10.1016/j.ssi.2015.01.002
8. Skodra A, Stoukides M (2009) Solid State Ion 180:1332–1336
9. Lan R, Irvine JTS, Tao SW (2013) Sci Rep 3:1145
10. Amar IA, Lan R, Tao SW (2014) J Electrochem Soc 161(6):H350–H354
11. Amar IA, Petit CTG, Mann G, Lan R, Skabara PJ, Tao SW (2014) Int J Hydrog Energy 39:4322–4330
12. Jeoung H, Kim JN, Yoo CY, Joo JH, Yu JH, Song KC, Sharma M, Yoon HC (2014) Korean Chem Eng Res 52:58–62
13. Amar IA, Petit CTG, Lan R, Mann G, Tao SW (2014) RSC Adv 4:18749–18754
14. Lan R, Alkhazmi KA, Amar IA, Tao SW (2014) Electrochim Acta 123:582–587
15. Abghoui Y, Garden AL, Hlynsson VF, Bjorgvinsdottir S, Olafsdottir H, Skulason E (2015) Phys Chem Chem Phys 17:4909–4918. doi:10.1039/c4cp04838e
16. Ouzounidou M, Skodra A, Kokkofitis C, Stoukides M (2007) Solid State Ion 178:153–159
17. Zhang Z, Zhong Z, Liu R (2010) J Rare Earths 28(4):556–559
18. Xu G, Liu R (2009) Chin J Chem 27:677–680
19. Lan R, Alkhazmi KA, Amar IA, Tao SW (2014) App Cat B 152–153:212–217
20. Skúlason E, Bligaard T, Gudmundsdóttir S, Studt F, Rossmeisl J, Abild-Pedersen F, Vegge T, Jónsson H, Norskov JK (2012) Phys Chem Chem Phys 14:1235–1245
21. Wang Z, Liu B, Lin J (2013) Appl Catal A 458:130–136
22. Vayenas CG, Bebelis S, Pliangos C, Brosda S, Tsiplakides D (2001) Electrochemical activation of catalysis. Kluwer Academic/Plenum, New York
23. Vayenas CG, Koutsodontis CG (2008) J Chem Phys 128:182506
24. Vayenas CG (2011) J Sol St Electrochem 15:14251435
25. Garagounis I, Kyriakou V, Stoukides M (2013) Sol St Ion 231:58–62
26. Marnellos G, Zisekas S, Stoukides M (2000) J Catal 193:80–87
27. Yiokari CG, Pitselis GE, Polydoros DG, Katsaounis AD, Vayenas CG (2000) J Phys Chem A 104(46):10600–10602
28. Wang WB, Cao XB, Gao WJ, Zhang F, Wang HT, Ma GL (2010) J Membr Sci 360:397–403
29. Nicole J, Comninellis C (2008) J Appl Electrochem 28:223–226
30. Falgairette C, Jaccoud A, Foti G, Comninellis C (1998) J Appl Electrochem 38:1075–1082
31. Foti G, Jaccoud A, Falgairette C, Comninellis C (2009) J Electroceram 23:175–179
32. Souentie S, Xia C, Falgairette C, Li YD, Comninellis C (2010) Electrochem Commun 12:323–326
33. Matanović I, Garzon FH, Henson NJ (2014) Phys Chem Chem Phys 16:3014–3026
34. Amar IA, Lan R, Petit CTG, Tao SW (2015) Int J Electrochem Sci 10:3757–3766